Korea-Australia Rheology Journal
Vol. 15, No. 2, June 2003 pp. 83-90

Electrokinetic flow and electroviscous effect in a charged slit-like microfluidic channel with nonlinear Poisson-Boltzmann field

Myung-Suk Chun* and Hyun Wook Kwak
Complex Fluids Research Team, Korea Institute of Science and Technology (KIST) PO Box 131, Cheongryang, Seoul 130-650, South Korea

(Received February 28, 2003; final revision received May 10, 2003)

Abstract

In cases of the microfluidic channel, the electrokinetic influence on the transport behavior can be found. The externally applied body force originated from the electrostatic interaction between the nonlinear Poisson-Boltzmann field and the flow-induced electrical field is applied in the equation of motion. The electrostatic potential profile is computed a priori by applying the finite difference scheme, and an analytical solution to the Navier-Stokes equation of motion for slit-like microchannel is obtained via the Green's function. An explicit analytical expression for the induced electrokinetic potential is derived as functions of relevant physicochemical parameters. The effects of the electric double layer, the zeta potential of the solid surface, and the charge condition of the channel wall on the velocity profile as well as the electroviscous behavior are examined. With increases in either electric double layer or zeta potential, the average fluid velocity in the channel of same charge is entirely reduced, whereas the electroviscous effect becomes stronger. We observed an opposite behavior in the channel of opposite charge, where the attractive electrostatic interactions are presented.

Keywords **:** electrokinetic flow, electrostatic interaction, electroviscous effect, microfluidic channel, navier-stokes equation, poisson-boltzmann equation

1. Introduction

An understanding of the fundamental behavior of the fluid flow in microchannels is of considerable importance in the research fields of micro- and nanofluidics. Microchannels currently have wide applications in the design and utilization of microfluidic devices, such as diagnostic microdevices, biomedical microchips, microreactors, and other MEMS (micro-electro mechanical system) devices (Manz *et al.*, 1994; Hu *et al.*, 1999; Weilin *et al.*, 2000). It should be noted that laminar flow is the definitive characteristic of microfluidics. Fluid flowing in microchannels with dimensions on the order of tens or hundreds of micrometers is characterized by low Reynolds number (Stone and Kim, 2001; Karniadakis and Beskok, 2002). Pressure-driven Poiseuille flow in a various type of channel is well understood, but the fluid flow behavior in charged microchannels is influenced by the electrokinetic effect and hence deviates from that described by the traditional form of the Navier-Stokes equation.

When a fluid is forced through a microchannel under an applied pressure, the counter-ions in the mobile part of the electric double layer (EDL) are carried toward the downstream end. Then an electric current called the streaming current results in the pressure-driven flow direction. Corresponding to this streaming current, there is an electrokinetic potential called the streaming potential. This flow-induced streaming potential acts to drive the counter-ions in the mobile part of the EDL to move in the direction opposite to the streaming current. This flow of ions in the opposite direction to the pressure-driven flow will generate conduction current. The overall result is a reduced flow rate in the direction of pressure drop. If the reduced flow rate is compared with the flow rate of uncharged inert case, it seems that the fluid would have a higher viscosity. This rheological aspect is usually referred to as the electroviscous effect. The effect of EDL is neglected, as the thickness of the EDL is quite small. However, the EDL effect cannot be neglected in the study of microchannel flow, where the EDL thickness is comparable with the characteristic size of the flow channel.

About forty years ago, the effect of the surface potential on fluid transport through narrow cylindrical capillary with the Debye-Hückel approximation was discussed and the electroviscous effect was also considered (Rice and Whitehead, 1965). Later, the same problem with higher surface potential was investigated by developing an approximate solution to the Poisson-Boltzmann (P-B) equation pertaining to an imposed electric field (Levine *et al.*, 1975). In

*Corresponding author: mschun@kist.re.kr
© 2003 by The Korean Society of Rheology

recent, the electroviscous effect on the electrokinetic flow velocity in rectangular channel was estimated by solving coupled equation of motion with P-B equation (Li, 2001; Ren *et al.*, 2001; Hsu *et al.*, 2002). For slit-like microchannel with a linearized P-B field, analytical solutions to the flow velocity and the flow-induced electrokinetic potential have been obtained by employing the Green's function, where characteristic length scale is less than tens of micrometers (Chun, 2002). Chun (2002) also pointed out a necessity of further analysis on the behavior of electrokinetic flows with respect to the nonlinear full P-B field.

In this study, both the electrokinetic flow behavior and the electroviscous effect in a slit-like microchannel are analyzed by applying the Green's function formulation. The electrostatic potential is firstly considered by solving the nonlinear P-B equation using the finite difference method (FDM), and then the equation of motion is developed by dealing with the external body force and the relevant flow-induced electrical field. We predict identically the electric potential profile as well as the velocity profile with variations of ionic concentration of solution, zeta potential, and charge condition of the channel wall. Finally, the electroviscous effect is estimated by obtaining the ratio of the apparent fluid viscosity to the inert bulk viscosity.

2. Flow field coupled with electrokinetic interaction

2.1. Flow through a charged slit-like channel

In principle, the Navier-Stokes equation furnishes the paradigm for describing the equation of motion for an incompressible ionic fluid, given by

$$\rho\frac{\partial \boldsymbol{v}}{\partial t}+\rho(\boldsymbol{v}\cdot\nabla)\boldsymbol{v}=-\nabla p+\boldsymbol{F}+\eta\nabla^2\boldsymbol{v} \tag{1}$$

where ρ and η are the density and viscosity of the fluid, respectively. Let us consider the one-dimensional laminar flow through a slit-like channel, then $\boldsymbol{v}=[0,\ 0,\ v_z(y)]$ is taken with Cartesian coordinates (Happel and Brenner, 1983). Neglecting gravitational forces, the body force per unit volume F ubiquitously caused by the z-directional action of an induced electrical field E_z on the net charge density ρ_e can be written $F_z=\rho_e E_z$. With these identities, Eq. (1) is reduced to

$$\eta\frac{d^2v}{dy^2}=\frac{dp}{dz}-\rho_e E_z \tag{2}$$

In view of taking a flow only in the z-direction in a slit spaced a distance 2H apart, the velocity profile known as a plane Poiseuille flow is obtained as $v_z=(H^2/2\eta)(dp/dz)[1-(y/H)^2]$. The ρ_e for the full P-B electric field is described in Section 3. One obtains the nondimensionalized equation of motion, such that

$$\frac{d^2V}{dY^2}=\frac{dP}{dZ}+\Gamma_1 E\sinh\Psi \tag{3}$$

with the following dimensionless parameters

$$Z=\frac{z}{d_h Re},\quad Y=\frac{y}{d_h},\quad V=\frac{v}{U},\quad Re=\frac{\rho d_h U}{\eta},\quad P=\frac{p}{\rho U^2},$$
$$E=\frac{E_z d_h Re}{\psi_o},\quad \Gamma_1=\frac{2z_i e n_b \psi_o}{\rho U^2} \tag{4}$$

where d_h means the hydraulic diameter (i.e., $4H$), U the reference velocity, and ψ_o the reference electrical potential. The boundary conditions are applied as

$$V=0 \quad \text{at} \quad Y=\frac{H}{d_h}, \tag{5a}$$

$$\frac{dV}{dY}=0 \quad \text{at} \quad Y=0. \tag{5b}$$

The Green's function formulation with the differential operator L, which is described in the reference books (see, e.g., Arfken, 1985), can be used for $V(Y,t)$ as follows

$$LV=\left[\eta\frac{\partial}{\partial t}-\frac{\partial^2}{\partial Y^2}\right]V=-\frac{\partial P}{\partial Z}-E\Gamma_1\sinh\Psi(Y) \tag{6}$$

Solution of this equation proceeds by standard techniques. We here consider the Green's function as a linear combination of the eigenvalues and corresponding eigenfunctions ϕ_n, established as

$$G(Y,Y',t)=\sum_n^{\infty} e^{-\beta_n t}\phi_n(Y)\phi_n(Y') \tag{7}$$

where t is normalized by $\rho d_h^2/\eta$, and a convenient representation for the eigenvalues $\beta_n=[(2n-1)\pi d_h/2H]^2$. Utilization of the Dirac delta function with orthogonal properties leads to the following expression

$$LG(Y,Y',t)\equiv\delta(Y-Y')\delta(t) \tag{8}$$

Then, the solution of Eq. (6) subjecting to the above boundary conditions is given by

$$V(Y,t)=\int_0^t dt'\int_0^{H/d_h} dY' G(Y,Y',t-t')\left[-\frac{dP}{dZ}-E\Gamma_1\sinh\Psi(Y')\right] \tag{9}$$

The Green's function is explicitly found by using the separation of variables method, yielding

$$G=\frac{d_h}{H}\sum_{n=1}^{\infty} e^{-\frac{(2n-1)^2\pi^2 d_h^2}{4H^2}t}\cos\frac{(2n-1)\pi d_h}{2H}Y\cos\frac{(2n-1)\pi d_h}{2H}Y' \tag{10}$$

The solution for velocity profile yields as

$$V(Y,t)=\frac{d_h}{H}\sum_{n=1}^{\infty}\lim_{t\to\infty}\int_0^t dt' e^{-\beta_n(t-t')}\int_{-H/d_h}^{H/d_h} dY'\cos\sqrt{\beta_n}Y\cos\sqrt{\beta_n}Y'$$
$$\times\left[-\frac{dP}{dZ}-E\Gamma_1\sinh\Psi(Y')\right]. \tag{11}$$

Both integrating and rearranging give the velocity profile as follows,

$$V(Y)=\frac{2d_h}{H}\sum_{n=1}^{\infty}\left(\frac{\cos\sqrt{\beta_n}Y}{\beta_n}\right)\left[\frac{(-1)^n dP}{\sqrt{\beta_n}\,dZ}\right.$$
$$\left.-\frac{E\Gamma_1}{2}\int_{-H/d_h}^{H/d_h}dY'\cos\sqrt{\beta_n}Y'\sinh\Psi\right]$$
$$=V_{inert}(Y)-\frac{d_h}{H}\sum_{n=1}^{\infty}\left(\frac{\cos\sqrt{\beta_n}Y}{\beta_n}\right)E\Gamma_1\int_{-H/d_h}^{H/d_h}dY'\cos\sqrt{\beta_n}Y'\sinh\Psi \quad (12)$$

where V_{inert} is the velocity profile in the absence of the electrostatic interaction, that equals to the plane Poiseuille flow profile. Ultimately, the average fluid velocity is obtained as

$$\langle V\rangle=\frac{\int_0^{H/d_h}dYV}{\int_0^{H/d_h}dY}=-\frac{2d_h^2}{H^2}\sum_{n=1}^{\infty}\frac{1}{\beta_n^2}\frac{dP}{dZ}+\frac{d_h^2}{H^2}E\Gamma_1\sum_{n=1}^{\infty}\frac{(-1)^n}{\beta_n^{3/2}}\times$$
$$\int_{-H/d_h}^{H/d_h}dY'\cos\sqrt{\beta_n}Y'\sinh\Psi=-\langle V\rangle_{inert}+\frac{d_h^2}{H^2}E\Gamma_1\sum_{n=1}^{\infty}\frac{(-1)^n}{\beta_n^{3/2}}\times$$
$$\int_{-H/d_h}^{H/d_h}dY'\cos\sqrt{\beta_n}Y'\sinh\Psi \quad (13)$$

2.2. Flow-induced electrokinetic potential (streaming potential)

As derived in Eq. (3), both the local velocity and the average fluid velocity can be calculated when the nondimensional induced electrical field E is known. Ions from the double layer region are transported along with the streaming solution, resulting in a streaming current I_s, in the direction of flow. The resultant induced electrokinetic potential, which is generally called the streaming potential E_z, then induces a flow of ions in the opposite direction known as the electrical conduction current I_c. When the flow reaches a steady state, the summation of the streaming and conduction current should be zero, so that

$$\nabla\cdot I=I_s+I_c\equiv 0. \quad (14)$$

The streaming current I_s caused by the pressure-driven liquid flow is called the electrical convection current. For a slit-like microchannel with the specified width W, it is defined by

$$I_s=Wd_hU\int dY\rho_e V$$
$$=\frac{Wd_h^2U\varepsilon\kappa^2}{H}\int_{-H/d_h}^{H/d_h}dY\sinh\Psi\times$$
$$\left[\sum_{n=1}^{\infty}\frac{\cos\sqrt{\beta_n}Y}{\beta_n}\left(\frac{2}{\sqrt{\beta_n}}(-1)^n\frac{dP}{dZ}-E\Gamma_1\int_{-H/d_h}^{H/d_h}dY'\cos\sqrt{\beta_n}Y'\sinh\Psi\right)\right]. \quad (15)$$

The electrical conduction current I_c can be expressed as

$$I_c=\lambda_t E_z(2HW)=\lambda_t\frac{E\psi_o}{d_hRe}(2HW) \quad (16)$$

where λ_t is the total electrical conductivity and $2HW$ is the cross-sectional area of the channel. Note that the electrical conduction current consists of bulk electrical conductivity and surface electrical conductivity. The bulk conductivity of the monovalent symmetric electrolyte system (e.g., NaCl, KCl solution) is almost much greater than the surface conductivity of the channels made on inorganic or polymeric materials (Chun *et al.*, 2002). In this respect, the λ_t in this study can be determined by the value of the bulk conductivity. Substituting Eqs. (15) and (16) into Eq. (14), the nondimensional induced electrokinetic potential E is derived as

$$E=\frac{\frac{2d_h^2\varepsilon\kappa^2U}{H}\int_{-H/d_h}^{H/d_h}dY\sinh\Psi\left(\sum_{n=1}^{\infty}\frac{\cos\sqrt{\beta_n}Y}{\beta_n^{3/2}}(-1)^n\frac{dP}{dZ}\right)}{\left\{\frac{2H\psi_o\lambda_t}{d_h^2Re}+\frac{d_h^2U\varepsilon\kappa^2\Gamma_1}{H}\int_{-H/d_h}^{H/d_h}dY\sinh\Psi\times\left(\sum_{n=1}^{\infty}\frac{\cos\sqrt{\beta_n}Y}{\beta_n}\int_{-H/d_h}^{H/d_h}dY'\cos\sqrt{\beta_n}Y'\sinh\Psi\right)\right\}} \quad (17)$$

With defining the dimensionless variable $\Gamma_2=2z_ien_bd_hU/\lambda_t\psi_o$, Eq. (17) can be expressed as follows,

$$E=\frac{\frac{d_h^2\Gamma_2Re}{H^2}\int_{-H/d_h}^{H/d_h}dY\sinh\Psi\left(\sum_{n=1}^{\infty}\frac{\cos\sqrt{\beta_n}Y}{\beta_n^{3/2}}(-1)^n\frac{dP}{dZ}\right)}{\left\{1+\frac{d_h^2\Gamma_1\Gamma_2Re}{2H^2}\int_{-H/d_h}^{H/d_h}dY\sinh\Psi\times\left(\sum_{n=1}^{\infty}\frac{\cos\sqrt{\beta_n}Y}{\beta_n}\int_{-H/d_h}^{H/d_h}dY'\cos\sqrt{\beta_n}Y'\sinh\Psi\right)\right\}} \quad (18)$$

2.3. Electroviscous effect

As described above, the streaming potential E produces a liquid flow in the direction opposite to the pressure-driven flow. The flow rate through the microchannel with and without the consideration of the EDL effects can be considered from Eq. (13). Then, one may obtain the ratio of the apparent fluid viscosity to the inert bulk viscosity as follows:

$$\frac{\eta}{\eta_{inert}}\equiv\frac{\langle V\rangle_{inert}}{\langle V\rangle}=\frac{1}{1-\frac{E\Gamma_1}{2}\frac{\sum_{n=1}^{\infty}\frac{(-1)^n}{\beta_n^{3/2}}\int_{-H/d_h}^{H/d_h}dY'\cos\sqrt{\beta_n}Y'\sinh\Psi}{\sum_{n=1}^{\infty}\frac{1}{\beta_n^2}\frac{dP}{dZ}}} \quad (19)$$

where it is easy to show that this ratio is greater than 1.

3. Nonlinear Poisson-Boltzmann electric field with finite difference scheme

When the charged surface is contact with an electrolyte,

the electrostatic charge would influence the distribution of nearby ions so that an electric field is established. The charges on the solid surface and the balancing charges in the liquid consist of both the compact double layer referred to as the Stern layer and the diffuse layer (Hunter, 1981; Russel *et al.*, 1989). In order to compute the velocity profile and the electroviscous effect in a charged microchannel, the electric potential ψ should be evaluated. The nonlinear P-B equation governing the electric field is given as

$$\nabla^2\Psi = \kappa^2 \sinh\Psi \tag{20}$$

Here, the dimensionless potential Ψ denotes $z_i e\psi/kT$ and the inverse Debye length (i.e., inverse EDL thickness) κ is defined by

$$\kappa = \left[\frac{2n_{i,b}z_i^2 e^2}{\varepsilon kT}\right]^{1/2} \tag{21}$$

where z_i is the valence of type i ions, e the elementary charge, ε the dielectric constant, and kT the Boltzmann thermal energy. In Eq. (21), $n_{i,b}$ is the concentration of type i ions in the bulk solution, where $n_{i,b}$ ($1/m^3$) equals to a product of Avogadros number and ionic strength C_b (mM). For low potential of $\Psi \leq 1$ (i.e., less than $kT/e = 25.69$ mV) with 1:1 electrolyte system, the P-B equation may be linearized, that is called the Debye-Hückel equation. The application scope of this linearized P-B field is narrow in real situations, because the surface potentials favorably have values larger than 25.69 mV.

We consider a slit-like channel confined between parallel planes of width 2H, then dimensionless nonlinear P-B equation leads to

$$\frac{\partial^2\Psi}{\partial Y^2} = (\kappa d_h)^2 \sinh\Psi \tag{22}$$

The following boundary conditions are presented in a half of the channel cross-section,

$$\Psi = \Psi_s \quad \text{at } Y=0 \text{ and } \frac{H}{d_h} \tag{23}$$

To obtain the solution of Eq. (22) with the boundary conditions, taking five-point central difference method yields the left-hand side of Eq. (22) as

$$\frac{\partial^2\Psi}{\partial Y^2} = \frac{\Psi_{j+1}^{k+1} - 2\Psi_j^{k+1} + \Psi_{j-1}^{k+1}}{(\Delta Y)^2} \tag{24}$$

where k means the iteration index and the grid index $j = 1,2, \ldots N$. The functions on the right-hand side of Eq. (22) can be linearized as

$$\sinh\Psi_j^k = \sinh\Psi_j^k + (\Psi_j^{k+1} - \Psi_j^k)\cosh\Psi_j^k \tag{25}$$

Substituting Eqs. (24) and (25) into Eq. (22), the finite difference form of the nonlinear P-B equation becomes as follows

$$\frac{\Psi_{j+1}^{k+1} - 2\Psi_j^{k+1} + \Psi_{j-1}^{k+1}}{(\Delta Y)^2} = \kappa^2[\sinh\Psi_j^k + (\Psi_j^{k+1} - \Psi_j^k)\cosh\Psi_j^k] \tag{26}$$

Then, Eq. (26) is rewritten, like as

$$\Psi_{j+1}^{k+1} - (2 + (\Delta Y)^2\kappa^2\cosh\Psi_j^k)\Psi_j^{k+1} + \Psi_{j-1}^{k+1} = (\Delta Y)^2\kappa^2(\sinh\Psi_j^k - \Psi_j^k\cosh\Psi_j^k) \tag{27}$$

Eq. (27) can be solved for Ψ_j^{k+1} by successive iterative calculation, using the value of Ψ obtained in the k-th iteration (Gerald and Wheatley, 1992). A series of algebraic equations can be expressed as a matrix form, given by

$$\boldsymbol{A}\cdot\boldsymbol{x} = \boldsymbol{b} \tag{28}$$

where

$$\boldsymbol{A} = \begin{bmatrix} P(\Psi_1^k) & 1 & 0 & \cdots & \cdots & 0 \\ 1 & P(\Psi_2^k) & 1 & & \iddots & \vdots \\ 0 & 1 & \ddots & \ddots & & \vdots \\ \vdots & & \ddots & \ddots & 1 & 0 \\ \vdots & \iddots & & 1 & P(\Psi_{N-1}^k) & 1 \\ 0 & \cdots & \cdots & 0 & 1 & P(\Psi_N^k) \end{bmatrix} \tag{29}$$

$$\boldsymbol{x}^T = [\Psi_1^{k+1},\ \Psi_2^{k+1},\ \cdots,\ \Psi_j^{k+1},\ \cdots,\ \Psi_{N-1}^{k+1},\ \Psi_N^{k+1}] \tag{30}$$

$$\boldsymbol{b}^T = [Q(\Psi_1^k) - \Psi_s, Q(\Psi_2^k), \cdots, Q(\Psi_j^k), \cdots, Q(\Psi_{N-1}^k), Q(\Psi_N^k) - \Psi_s] \tag{31}$$

In Eqs. (29) and (31), the constant potential boundary condition takes the following form

$$P(\Psi) = -2 - (\Delta Y)^2\kappa^2\cosh\Psi \tag{32}$$

$$Q(\Psi) = (\Delta Y)^2\kappa^2(\sinh\Psi - \Psi\cosh\Psi) \tag{33}$$

Once the electric potential profile is obtained, it is straightforward to determine the local net charge density as follows

$$\rho_e = z_i e(n_+ - n_-) = -2z_i e n_{i,b}\sinh\Psi \tag{34}$$

4. Results and discussion

For illustrative computations, we consider a fully developed laminar flow of an aqueous NaCl solution through a slit-like microchannel made on inorganic materials such as fused silica. The channel width 2H is chosen to be 2 μm. The ionic concentration of 1:1 type electrolyte equals to the ionic strength of the solution. At room temperature, the dielectric constant and the viscosity of the fluid are taken as $\varepsilon = 80 \times (8.854 \times 10^{-12})$ Coul/N·m^2 and $\eta = 1.0 \times 10^{-3}$ kg/m·sec, respectively. The bulk conductivity with variations of ionic concentrations is chosen from the literature value (Lide, 1999; Chun, 2002). The finite difference grids of 1000 are built within the channel, and the convergence criterion is given as 10^{-5}. All computations performed on an IBM PC with Pentium IV processor (1.5 GHz) take less than 1 minute.

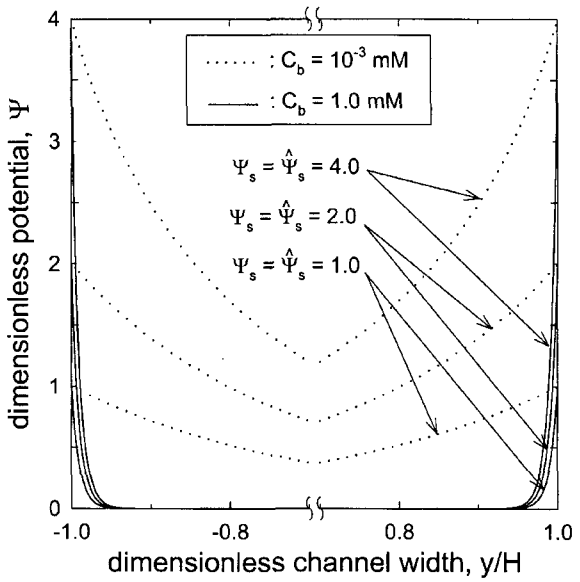

Fig. 1. Potential profile in a same charged slit-like microchannel for several solution ionic concentrations (i.e., Debye length) as well as surface potentials.

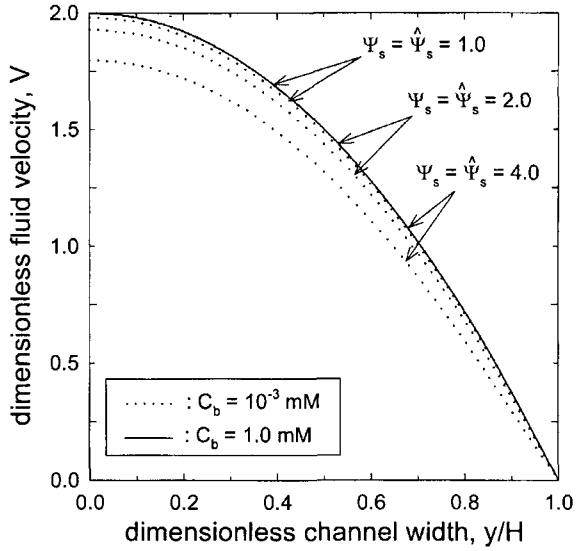

Fig. 2. Velocity profile in a same charged slit-like microchannel for several solution ionic concentrations (i.e., Debye length) as well as surface potentials, where $C_b = 10^{-3}$ mM and pressure gradient dp/dz is 1.0×10^5 N/m^3.

4.1. Electric potential and velocity profiles

In the microchannel, the inner surfaces of both the lower wall and the upper wall have surface potentials of Ψ_s and $\hat{\Psi}_s$, respectively. It is possible to assume here that the surface potential is identical to the zeta potential. A decrease of NaCl electrolyte concentration C_b corresponds to an increase of Debye length κ^{-1}, which provides a measure of the range of the long-range electrostatic interactions. Since the double layer thickness κ^{-1} (nm) equals to $[C_b(\mathrm{M})]^{-1/2}$/ 3.278 for 1:1 type electrolytes, the ionic strengths of 1.0 and 10^{-3} mM correspond to the κ^{-1} of 9.7 and 305 nm, respectively.

As shown in Fig. 1, the potential profile moves toward the center region as the surface potential increases. Getting far from the surface of the channel wall, the potential is decreased and the EDL thickness can be determined. An increase in the long-range repulsive screened electrostatic interaction with increasing the surface potential is more dramatic for lower solution ionic strength. Given the potential profile, the velocity profile can subsequently be computed by using Eq. (12). In Fig. 2, the EDL does not exhibit any effects on the flow pattern for the solution ionic strength of 1.0 mM. However, a dependency of the surface potential upon the velocity profile can distinctly be seen for the solution ionic strength of 10^{-3} mM.

Fig. 3 shows that the potential profiles are changed according to the charge condition of the wall surfaces. When each of the wall surfaces has opposite charge, the electrostatic attraction is experienced. The charge condition of the wall surfaces also affects the velocity profile as given in Fig. 4. As the electrostatic attraction increases, the maximum velocity in the center of the channel is increased.

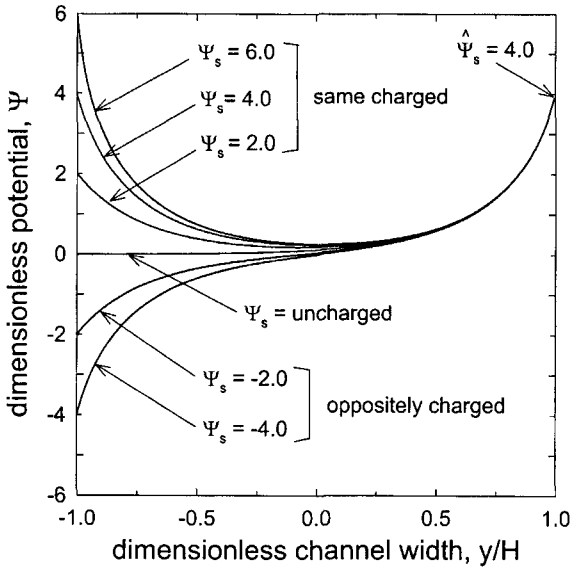

Fig. 3. Potential profile in both same and oppositely charged slit-like microchannels for several solution ionic concentrations (i.e., Debye length) as well as surface potentials, where $C_b = 10^{-3}$ mM.

Once each of the wall surfaces has opposite charge with equivalent magnitude of the potential, then the velocity profile becomes the Poiseuille flow.

4.2. Average velocity and electroviscous effect

It points out that the flow situations are verified as a low Reynolds number condition, which is certainly less than 1. In Fig. 5, the average fluid velocity <v> is entirely reduced with the increase in surface potential as well as the

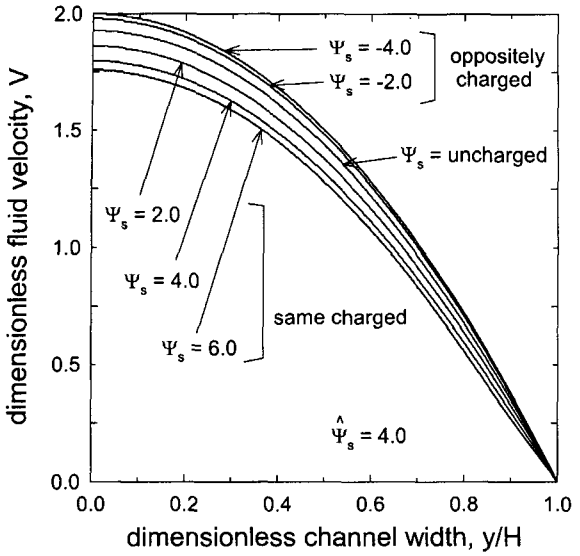

Fig. 4. Velocity profile in both same and oppositely charged slit-like microchannels for several solution ionic concentrations (i.e., Debye length) as well as surface potentials, where $C_b = 10^{-3}$ mM and pressure gradient dp/dz is 1.0×10^5 N/m^3.

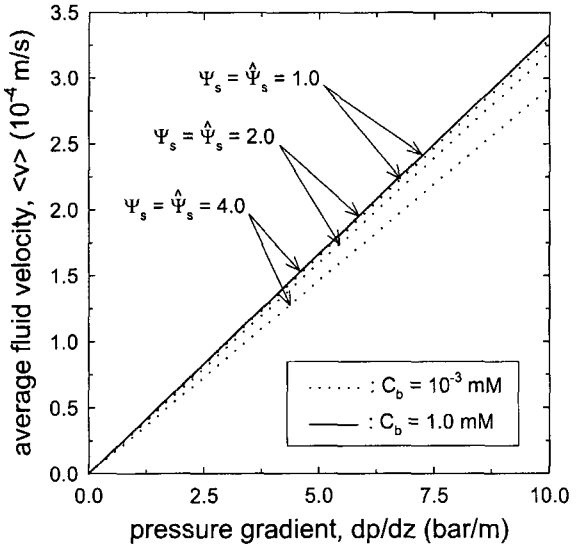

Fig. 5. The variations of average fluid velocity <v> with pressure gradient at different solution ionic concentrations as well as surface potentials, where the slit walls have same charge.

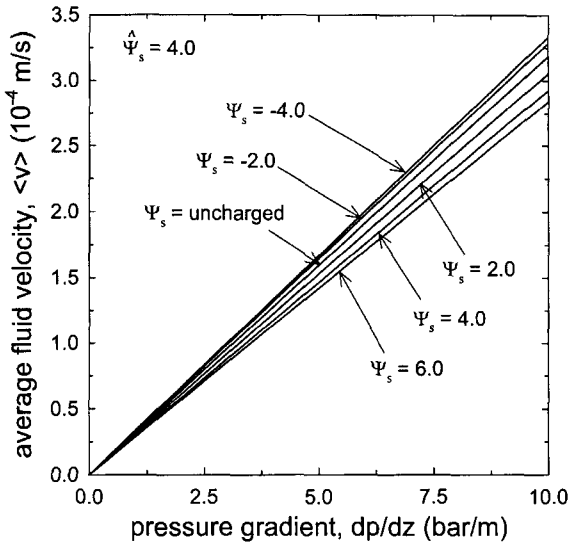

Fig. 6. The variations of average fluid velocity <v> with pressure gradient at different solution ionic concentrations as well as surface potentials, where the slit walls have both same and opposite charges and $C_b = 10^{-3}$ mM.

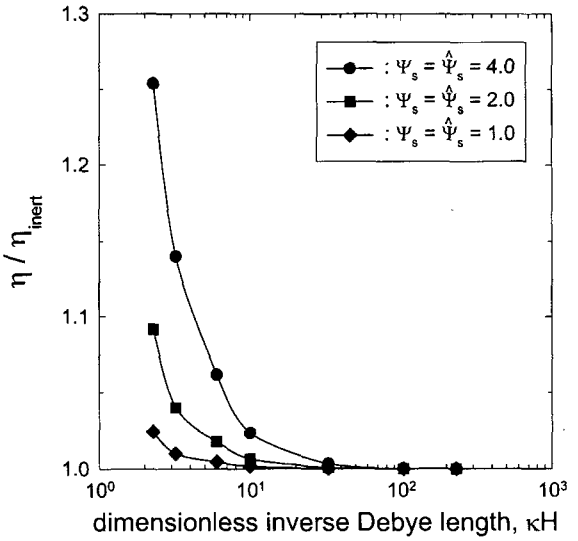

Fig. 7. The electroviscous effect with variations of dimensionless inverse Debye lengths (κH) and surface potentials, where the slit walls have same charge.

decrease in solution ionic strength. As described before, the charge concentration difference between the upstream and the downstream results in an induced electrokinetic potential, namely streaming potential. Therefore, a larger pressure gradient will generate a larger volume transport, a higher charge accumulation as well as a stronger induced electrical field will occur. The induced electrical field increases as the ionic concentration of the aqueous solution for a given pressure gradient decreases, due to a larger EDL thickness. This behavior leads us to understand the electrokinetic effect on the fluid velocity in microchannels. As shown in Fig. 6, the fluid velocity increases in accordance with increasing of the effect of opposite charge. This is due to a fact that the opposite charge generates the opposite streaming current, which would decrease the net streaming current through the channel, resulting reduction of the corresponding conduction current.

The electroviscous effect results from the moving ions in the diffuse layer which drag the surrounding liquid molecules. Hence, the viscosity enhancement associating a

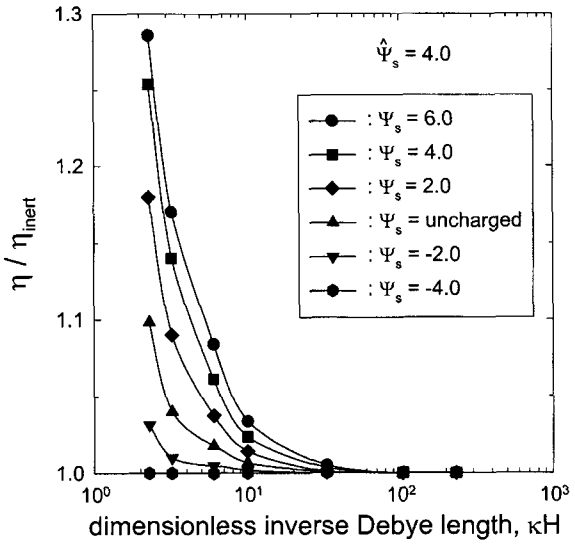

Fig. 8. The electroviscous effect with variations of dimensionless inverse Debye lengths (κH) and surface potentials, where the slit walls have both same and opposite charges.

rheological property can be estimated from the ratio of the fluid viscosity of charged case to that of inert case. In Fig. 7, the electroviscous effect increases with the increases of the Debye length (i.e., a decrease of the solution ionic strength) as well as the surface potential. The effect of charge condition shown in Fig. 8 corresponds to the feature of velocity profile provided in Fig. 4. It is evident that the electroviscous effect becomes weakened for the case of oppositely charged wall. A reduction of the conduction current due to the opposite charge gives rise to a decrease in the electroviscous effect.

5. Conclusions

Recently, a microchannel analysis of the requisite microfluidic problems has been usefully confronted. The main thrust of the present study is an analysis on the electrokinetic flow of ionic fluids in slit-like microchannels. The additional body force originated from the presence of the nonlinear P-B electric field and the flow-induced electrical field was considered in the equation of motion. Applying the Green's function formula could derive the expressions in explicit forms for the velocity profile, the induced electrokinetic potential, and the electroviscous effect as functions of relevant parameters.

Theoretical results emphasize that the velocity profile is clearly affected by the EDL for the cases of low ionic concentrations and high zeta potentials, where the average fluid velocity decreases as the solution ionic concentration decreases. Since both the EDL and the induced electrokinetic potential act against the liquid flow, they result in a reduced flow rate and this behavior is directly related to the electroviscous effect. We also examined the influence of the surface charge condition upon both the potential and the velocity profiles. Compared to the case of same charge, the channel walls of opposite charge display an opposite behavior on the average fluid velocity as well as the electroviscous effect.

Acknowledgements

This work was supported by the Basic Research Fund (Grant No. R01-2001-000-00411-0) from the Korea Science and Engineering Foundations (KOSEF). The Future-Oriented Research Fund (2E17460) from the KIST was also partially supported.

Nomenclature

C_b	: solution ionic strength [M]
d_h	: hydraulic diameter [m]
E	: dimensionless induced electrokinetic potential, or streaming potential [–]
E_z	: dimensional E [V/m]
e	: elementary charge [Coul]
F	: body force [N/m^3]
H	: half channel width [m]
I	: net electrical current [A]
I_c	: electrical conduction current [A]
I_s	: electrical convection current [A]
kT	: Boltzmann thermal energy [J]
$n_{i,b}$	: concentration of charged ions [1/m^3]
P	: dimensionless hydraulic pressure [–]
p	: hydraulic pressure [N/m^2]
Re	: Reynolds number [–]
t	: dimensionless time [–]
U	: reference velocity [m/s]
V	: dimensionless fluid velocity [–]
$\langle V \rangle$	: dimensionless average fluid velocity [–]
v	: fluid velocity component [m/s]
W	: specified width [m]
Y	: non-dimensional lateral (y-) coordinate [–]
Z	: non-dimensional axial (z-) coordinate [–]
z_i	: valence of ion [–]

Greek Letters

β_n	: set of eigenvalues [–]
ε	: dielectric constant [Coul^2 /J · m]
ϕ_n	: set of eigenfunctions [–]
κ	: inverse Debye length, or inverse EDL thickness [1/m]
ρ	: fluid density [kg/m^3]
ρ_e	: net charge density [Coul/m^3]
η	: fluid viscosity [kg/m · s]
η_{inert}	: fluid viscosity of inert case [kg/m · s]
Γ_1, Γ_2	: non-dimensional parameters [–]

λ_t : total electrical conductivity [$1/\Omega \cdot m$]
Ψ : dimensionless electrostatic potential [–]
Ψ_s : dimensionless electrostatic surface potential [–]
$\hat{\Psi}_s$: dimensionless electrostatic surface potential of opposing wall [–]
ψ_o : reference electrical potential [V]

Mathematical

$\boldsymbol{A}$: finite difference matrix [–]
$\boldsymbol{b}$: finite difference vector [–]
G : Green's function [–]
L : differential operator [–]
$\boldsymbol{x}$: solution vector [–]
δ : Dirac delta function [–]

References

Arfken, G., 1985, Mathematical Methods for Physicists, 3rd Ed., Academic Press, New York.

Chun, M.-S., 2002, Electrokinetic Flow Velocity in Charged Slit-like Microfluidic Channels with Linearized Poisson-Boltzmann Field, *Korean J. Chem. Eng.* **19**, 729-734.

Chun, M.-S., H.I. Cho and I.K. Song, 2002, The electrokinetic behavior of membrane zeta potential during the filtration of colloidal suspensions, *Desalination* **148**, 363-368.

Gerald, C.F. and P.O. Wheatley, 1992, Applied Numerical Analysis, 4th Ed., Addison-Wesley, Tokyo.

Happel, J. and H. Brenner, 1983, Low Reynolds number hydrodynamics: with special applications to particulate media, Martinus Nijhoff, Hague.

Hsu, J., C. Kao, S. Tseng and C. Chen, 2002, Electrokinetic Flow through an Elliptical Microchannel: Effects of Aspect Ratio and Electrical Boundary Conditions, *J. Colloid Interface Sci.* **248**, 176-184.

Hu, L., D.J. Harrison and J.H. Masliyah, 1999, Numerical model of electrokinetic flow for capillary electrophoresis, *J. Colloid Interface Sci.* **215**, 300-312.

Hunter, R.J., 1981, Zeta Potential in Colloid Science: Principles and Applications, Academic Press, New York.

Karniadakis, G.E. and A. Beskok, 2002, Micro Flows: Fundamentals and Simulation, Springer-Verlag, New York.

Levine, S., J.R. Marriott, G. Neale and N. Epstein, 1975, Theory of Electrokinetic Flow in Fine Cylindrical Capillaries at High Zeta-Potentials, *J. Colloid Interface Sci.* **52,** 136-149.

Li, D., 2001, Electro-viscous effects on pressure-driven liquid flow in microchannels, *Colloids Surfaces A* **195**, 35-57.

Lide, D.R.(Eds.), 1999, CRC Handbook of Chemistry and Physics, 80th Ed., CRC Press, FL.

Manz, A., C.S. Effenhauser, N. Burggraf, D.J. Harrison, K. Seller and K. Flurl, 1994, Electroosmotic pumping and electrophoretic separations for miniaturized chemical analysis systems, *J. Micromech. Microeng.* **4**, 257-264.

Ren, L., D. Li and W. Qu, 2000, Electro-Viscous Effects on Liquid in Microchannels, *J. Colloid Interface Sci.* **233**, 12-22.

Rice, C.L. and R. Whitehead, 1965, Electrokinetic Flow in a Narrow Cylindrical Capillary, *J. Phys. Chem.* **69**, 4017-4024.

Russel, W.B., D.A. Saville and W.R. Schowalter, 1989, Colloidal Dispersions, Cambridge Univ. Press, New York.

Stone, H.A. and S. Kim, 2001, Microfluidics: Basic Issues, Applications, and Challenges, *AIChE J.* **47**, 1250-1258.

Weilin, Q., G.M. Mala and D. Li, 2000, Pressure-driven flows in trapezoidal silicon microchannels, *Int. J. Heat Mass Transfer* **43**, 353-364.